International Symposium of Research Students on Material Science and Engineering
December 20-22, 2004, Chennai, India
Department of Metallurgical and Materials Engineering, Indian Institute of Technology Madras

MICROSTRUCTURE EVALUATION OF MACHINABLE MICA BASED GLASS CERAMICS FOR DENTAL APPLICATION

Shibayan Roy
Dept. of Materials & Metallurgical Engg., IIT Kanpur

ABSTRACT

Machinable mica based glass ceramic materials with fluorophlogopite as the main crystalline phase in the system K_2O-B_2O_3-Al_2O_3-SiO_2-MgO-F becomes the candidate material for the CAD-CAM dental restoration purpose. In our study, critical heat treatment experiments on this system in the varying temperature range of 1000°-1120°C with 40°C temperature interval for 4 hrs constant soaking time were carried out. Additionally experiments at 1000°C for varying soaking time of 4-24 hours with 4 hrs time interval were also carried out. Heating rate remains constant at 3.5°C/min for both the cases. The microstrctural changes are observed using optical microscopy, DTA, SEM-EDS, XRD etc. Furthermore, the microhardness of both these batches are measured using Vickers microhardness tester and correlated with the crystal volume fraction. For temperature variation batches, usual and already reported microstructure of interlocked, randomly oriented mica plates are seen. For time variation batches, an important and new observation is that the crystalline phase has a characteristic 'butterfly' like pattern i.e. mica rods are radiating from a central nucleus on both sides which is not reported yet. The possible mechanism for the development of this unusual microstructure is investigated.

KEY WORDS: Machinable Glass Ceramics, Mica, Microstructure, Microhardness, Crystal Volume fraction, Fluorophlogopite

1. INTRODUCTION:

Glass ceramics are polycrystalline materials prepared by the controlled crystallization of highly viscous glass-forming melts. Their properties depend on the amount and composition of crystal phase formed and also on the residual glass composition. [1]Again the crystal phase formation is a strong function of heat treatment time, temperature, heating rate, presence of nucleating agent, impurity etc. Glass ceramic materialsare already used in several applications as engineering materials and new uses constantly appear. The pioneer work of Larry L. Hench [2] showed that the glass ceramics can also be used for biomedical purpose including dental materials field. An important group of these materials i.e. the mica-containing glass-ceramics receive wide application due to their high machinability, which results in an increased versatility of the products and numerous possibilities for industrial application. Their potential use till date are in electronic/semiconductor Industry (precision coil formers & high voltage insulators), laser industry (spacers, cavities and reflectors in laser assemblies), high vacuum industry (thermal breaks in high temperature processing equipment, coil supports and vacuum feedthroughs), aerospace/space Industry (retaining rings on hinges, windows and doors of NASA's space shuttle, supports and components in several satellite borne systems) and in nuclear industry (fixtures and reference blocks in power generation units). The crystal phase generated in the mica containing glass ceramics is called fluorophlogopite ($KMg_3AlSi_3O_{10}F_2$) which is a trioctahedral fluoromica (Fig.2). It is basically composed of 2:1 negatively charged layers that are connected via large, positively charged interlayered alkali ions (Na and K, respectively).[16] A 2:1 sheet consists of two tetrahedral layers of the composition T_2O_5 (with ½ T=Al and $^3/_2$T= Si) and one octahedral layer possessing a hexagonal or pseudohexagonal arrangement of octahedral. A glass ceramic is considered machineable if it can be turned, milled, drilled and tapped, with the same (primarily carbide) tools as used for machining metals, without breaking

as normal ceramics would.[3] These glass ceramic materials consists of highly interlocked mica crystals, embedded in a glass matrix, facilitate microfracture along the weak mica-glass interfaces and mica basal planes, avoiding macroscopic failure during machining.[4] Due to, the contacts amongst the mica crystals, microfractures easily propagate from crystal to crystal, eventually resulting in material removal without breaking the part. The [001] plane of the mica crystal is preferred as a direction of fracture because the alkali ions sandwiched between the three-layer packets do not establish a compact connection.[3] Lawn et al [5] showed that for these materials, during Hertzian contact, deformation occurs in the form of an expanding microcrack damage zone instead of the usual single propagating microcrack for common brittle ceramics On this context, these glass ceramics materials appear to be a candidate material for fabricating dental restorations, as the main problem of all the dental ceramics is the premature failure during in vivo operational conditions due to the presence of surface flaws or cracks resulting during complex CAD/CAM operation.[4] Thompson et al [6] shows that Corning MGC is superior in terms of hardness and fracture toughness than Vita mark II which is mainly a dental porcelain, another leading material for dental use. Also Jedynakiewicz et al [7] demonstrated that when silicoated with $SiO_{(x)}$ and bonded to conventional composite luting agents, MGC showed a significantly higher adhesive assembly strength that that of porcelain.

In our present study, we have investigated the effect of varying crystallization temperature and time, keeping the heating rate constant, on the microstructure of the machinable mica based glass ceramics. Efforts were made to correlate between the volume fraction of characteristic crystal phase formed with the obtained microhardness.

2. MATERIALS AND METHOD

For our study, the commercial composition of MACOR® manufactured by the Corning Glass Ltd is used. This composition is obtained from the previous work of Guedes et al [8] and is rechecked from www.precisionceramics.co.uk . The composition is given in Table1 along with the raw materials used and their respective sources. All the starting powders are used in AR grade and they are around 99% pure with a very little impurity content. Base glass is prepared at 1500^{o}C in two steps i.e first the frit is being prepared by quenching the melt in water and then by remelting the frit and quenching in air. This is done for better homogenization of the constituent elements. The crystallization heat treatments are done both by varying temperature from 1000^{o}C to 1120^{o}C with 40^{o}C interval for 4hrs constant time duration and by varying time from 4 hrs to 24 hrs with 4hrs interval at constant temperature of 1000^{o}C. Heating rate remains constant at 3.5^{o}C/min for both the cases. Most of the past researchers e.g. Ma et al [9], Chen et al [10], Fischer-Cripps et al [11], Nagrajan et al [12], Gebhardt et al [13] etc had carried out the crystallization heat treatments in the temperature range of 1000^{o}C to 1120^{o}C, but no one has still done any time variation experiments on this temperature range. The reason for keeping the heat treatment temperature within this range is that the desired fluorophlogopite phase only formed in the range of 800^{o}C to nearly 1200^{o}C. [14] Bellow 800^{o}C, Aluminium Borate-Mullite solid solution crystals are formed whereas above 1100^{o}C, $MgAl_2O_4$ spinel is also present along with fluorophlogopite so that to get flurophlogopite alone, temperature should be kept within this range. After heat treatment, these samples were polished using Emery paper and Diamond paste (from 9 μm to 0.25 μm). They are etched with 12% HF and after an experiment of varying the etching time, 5 min is found to be suitable for revealing the microstructure. Furthermore the characterization of these samples is carried out using optical microscope, DTA, SEM-EDS, XRD etc. and microhardness is measured with a ZEISS microhardness tester at 160gm load. The optical and SEM images are analysised using Image Pro Plus software for crystal volume fraction calculation and surface plotting. SEM was done on *FEI QUANTA 200* machine whereas XRD was done on *Isodebyeflex 2002* machine and DTA was done in *PERKIN SPACE EIMER* machine. The total experimental procedure is schematically described bellow (Fig.3).

3: RESULTS AND DISCUSSIONS

3.1: MICROSTRUCTURE EVALUATION

XRD analysis of the heat treated samples was carried out in order to find out the possible crystal phases present. (Fig.5) Both the temperature variation and the time variation batches show the presence of flurophlogopite as the main crystalline phase. Samples heat treated at 1000^{o}C, 4hrs shows little sign of crystalinity in XRD results which can hardly be seen in the SEM micrographs [Fig.6 (a)]. May be the crystals are formed in a very small size which is not detectable in the background of large amount of glassy phase.

DTA of the base glass was carried in the temperature range of 40^{o}-1100^{o}C in order to find the crystallization temperature of different crystalline phases. From the DTA diagram of the base glass [Fig.4], it can be seen that the first crystal phase occurs at nearly 732^{o}C, which is evident from the large exothermic peak. In the crystallization process K_2O-Al_2O_3-SiO_2-MgO-B_2O_3-F system, first crystal phase to appear is the Aluminium Borate-Mullite solid solution crystal which on increasing temperature, transforms to fluorophlogopite on reaction with the matrix phase. The successive undulations in the diagram accounts for the generation of this crystalline phase and their continuous transformation to fluorophlogopite. The nucleation temperature of this first crystal is a strong function of heating rate as found by Bapna et al[15] and it was observed that with increasing heating rate shifts the nucleation temperature to a higher value. Heating rate during DTA is around 16.5^{o}C/min.

The other temperature variation samples e.g. 1040^{o}C, 1080^{o}C and 1120^{o}C shows the usual microstructure of straw like interlocked mica flakes randomly oriented in the glassy matrix. [Fig.6 (b)]. The interlocking is visible in Fig.6 (c) which shows the connectivity of the mica rods. It is because of this connectivity that these glass ceramics are machinable helping the microcracks to move along the weak interfaces from one mica rods to another. The random distribution of these mica rods over the whole glassy matrix can also be seen from the surface plots created by image analysis of the micrographs [Fig.7 (a)]. This “straw” like morphology of the characteristic mica crystal phase is very common and usual in the investigated glass - ceramic system and all the previous researchers like Habelitz et al[14], Hoche et al[16], Ma et al[9], Bapna et al[15], Cripps et al[11], Thompson et al[6] etc. have reported this kind of randomly oriented, interlocked microstructure. Another type of morphology of mica phase have been reported by some people like Vogel et al[3] and Gebhardt et al[13] which is called as “cabbage” shaped morphology. This occurs for slightly different base glass composition (21.2 mol. % MgO, 19.5 mol.Al_2O_3, 59.3 mol. % SiO_2 doped with 11.2 mol. % F^- and 6.4 mol. % Na_2O/K_2O) and at a heat treatment temperature lower than 1000^{o}C. Any other morphology of fluorophlogopite is not reported yet. In this context, the morphology of the crystal phase in time variation samples is unique in that it has a typical “butterfly” like shape with a number of mica rods radiating from a central point on both the two sides. [Fig.8 (a)] This morphology of the crystal phases is common for all the time variation batches. The individual mica rods are seen to be formed by the stacking of many mica plates which is actually snadwitched to form the mica rods. [Fig.8 (c)] At the end of each of the mica rods, a “tree leave” shaped structure is seen [Fig.8 (d)]. Small fragments of mica plate are found to be scattered all over the crystal phase and some glassy patches are seen over the crystals [Fig.8 (e) & (f)]. EDS analysis done on both the temperature and time variation batches shows the presence SiO_2 rich phase containing Al, Mg, O, K, B etc. in both “straw” like and “butterfly” like crystal phases as well as in the matrix of both temperature and time variation in almost similar quantity samples (Fig.9). In the time variation batches, for lower soaking time batches like 8hrs, 12hrs or 16 hrs, the crystal phases seems to be formed in some localized regions with large amount of spacing between each other. This is evident from the surface plots of these batches [Fig7 (b)]. As the soaking time increases more and more crystal phases are formed in different regions with their narrower spacing. In

samples having higher soaking time like 20hrs or 24 hrs, these crystals are seemed to have an overlapping structure and the glassy matrix is confined within a small isolated region (Fig.10).

The probable reason for the occurrence of this unique morphology of fluorophlogopite is related to the mechanism of crystal phase formation in this system. As we know, glass ceramic formation is governed by both temperature and time (Fig.11). Crystals start nucleating at lower temperature whereas higher temperature and time are required for growth of the existing crystals.[17] Higher temperature with lower time will facilitate more amount of nucleation than growth as higher temperature will help more and more embryos to cross the activation energy barrier and form tiny crystals. The growth of these existing crystals will not be large since lesser amount of time will restrict sufficient diffusion of materials. On the other hand, comparatively lower temperature with higher soaking time will help in growth of the existing crystals rather than formation of newer ones as diffusion is easy in this case rather than crossing of activation barrier. In the formation of crystals in the system of K_2O-Al_2O_3-SiO_2-MgO-B_2O_3-F, phase separation occurs at first and as small silica rich droplet phase with an enrichment of Mg, Al, alkali and fluorine ions in addition to silicic acid, is formed in the matrix phase which is very rich in SiO2 [3]. From this small silicate droplets, fluorophlogopite is produced on reaction with the matrix phase. The samples heat treated at 1000^{o}C for 4 hrs show little sign of detectable crystal formation. If we take it as the reference, on varying both temperature as well as time, we end up with crystalline samples with different morphologies. For temperature variation samples, higher temperature helps in the formation of greater number of small sized droplets and nucleation of large number of tiny crystals. But lower soaking time does not allow these crystals to grow much and randomly oriented "straw" like mica plates are being formed. On the other hand, a considerable number of nuclei are being formed for time variation batches but higher soaking time helps in their growth. Mica plates are continuously being formed from the glassy matrix and they are being deposited on the existing crystals. These plates are stacked together and form the mica rods on both the sides of the initial nuclei. From Fig.8 (a) & (b), it is quite evident that these crystals are formed from the spherical droplets. The "tree leave" like structure at the end of each rod is formed because the mica plates that are growing at those sites are not stacked to form the rod. The scattering of mica plates all over the crystal proves that mica plates are continuously being formed at different sites of the preexisting crystal. Also the glassy patches are the residual matrix from which mica plates are being formed. With increasing soaking time, more and more numbers of embryos can cross the activation barrier, thereby forming more amounts of crystal phases so that crystal volume fraction increases and crystals start overlapping with each other.

3.2. MICROHARDNESS AND CRYSTAL VOLUME FRACTION EVALUATION

The microhardness for the temperature variation samples is obtained to vary between 4.8 GPa to 5.5 GPa with samples heat treated at 1040^{o}C for 4 hrs showing the highest and the samples heat treated at 1080^{o}C for 4 hrs showing the lowest hardness. The hardness of the samples heat treated at 1120^{o}C for 4 hrs is in between these two values [Fig.12 (a)]. This observation is quite in agreement with the crystal volume fraction measurement with 1040^{o}C, 4hrs samples showing the highest amount of crystals of around 58% [Fig. 12 (b)]. The volume fraction of crystal phase does not vary much for the temperature variation samples and hardness values also have a narrow distribution. The indentations taken on these samples are quite clear in shape without any deformation of the sample [Fig.13] and are quite accurately measurable. This really indicates the phenemena of "quasi ductility" or machinability of these samples. For time variation samples, however, crystal volume fraction varies in a wide range from nearly 20% for 8 hrs soaking time batches to nearly 70% for 24 hrs batches [Fig.14 (a)]. The indentations are mostly taken on the crystal phases for these samples and it shows extensive localized deformation. The indentations are quite deformed in shape and an accurate measurement is very difficult [Fig15 (a) & (b)]. This kind of deformation of the crystal phase surely reflects more

brittleness of these "butterfly" crystals in time variation samples compared to temperature variation samples. This may have an effect in reducing the machinability of these time variation samples compared to temperature variation one.

4. CONCLUSION

The microstructural studies of temperature variation batches shows the usual randomly oriented, interlocked "straw" like mica plates, whereas time variation batches shows an unique "butterfly" shaped morphology of the crystal phase which is found to increase in number and overlap eventually as the soaking time increases. The mica rods are observed to radiate from the initial nucleus with the end of each rod having a "tree leave" like feature. The difference in these two morphologies possibly lies in the respective crystallization mechanisms. Wherein higher temperature helps more in nuclei formation, higher time helps in growth of the existing tiny crystals on both sides by the continuous formation and stacking of mica plates. Some more detailed studies like quantitative EDX analysis, compound identification using RAMAN spectroscopy, FTIR analysis i.e. more microstructural analysis in the temperature range of crystal formation in this system will surely lead us to a better understanding for the generation of this unusual crystal morphology. Microhardness measurements of temperature variation samples shows complete agreement with the volume fraction of crystal phase formed with highest volume fraction sample showing largest value of hardness. Hardness cannot be correlated with crystal volume fraction for the time variation batches and deformation at indentation sites reflects the more amount of brittleness of the "butterfly" crystals.

5. REFERENCES

1. Karamanov A, and Pelino M, *J. Euro. Cearam. Soc.* 19 (1999) 649-654
2. Hench L L, *J. Am. Ceram. Soc.* 81 [7] 1705-28 (1998)
3. Vogel W, Holand W, and Kaumann K, *J. Non-Crystal. Solids* 80 (1986) 34-51
4. Boccaccini A R, *j. Mat. Process. Tech.* 65 (1997) 302-304
5. Lawn B R, Padture N P, Cai H, and Guiberteau F, *Science* 263 (1994) 1114-1116
6. Thomson J Y, Bayne S C, and Heymann H O, *J. Prosthetic Dentistry* December (1994) 619-623
7. Jedynakiewicz N M, and Martin N, *Biomaterials* 22 (2001) 749-752
8. Guedes A, Pinto A M P, Vieira M, and Viana F, *Mat Sci. Engg A* 301 (2001) 118-124
9. Ma X P, Li G X, Shen L, and Jin Z H, *J. Am. Ceram. Soc.* 86 [6] 1040-42 (2003)
10. Chen X, Hench L L, Greenspan D, Zhong J, and Zhang X, *Ceram. Inter.* 24 (1998) 401-410
11. Cripps A C F, And Lawn B R, *Acta Mater*. 44 [2] 519-527 (1996)
12. Nagrajan V S, and Jahanmir S, *Wear* 200 (1996) 176-185
13. Gebhardt A, Hoche T, carl G, and Khoods I I, *Acta Mater* 47 [17] 4427-4434 (1999)
14. Habelitz S, hoche T, Hergt R, carl G, and Russel C, *Acta Mater* 47 [9] 2831-2840 (1999)
15. Bapna M S, and Mueller H J, *Biomaterials* 17 (1996) 2045-2052
16. Hoche T, Habelitz S, and Khood I I, *J. Crystal Growth* 192 (1998) 185-195
17. Mcmillan P W, "*Glass-Ceramics*", Academic Press, London and New York, 1964, p 37

TABLES

Table1: Composition of base glass

Starting Materials	Oxide Constituent	Wt %	Comments
Silica Gel in powder form	SiO_2	46	60-120 mesh, AR grade
White Tabular Alumina	Al_2O_3	16	99.9% pure, d_{50}= <1µm, AR grade
MgO powder	MgO	17	99% pure, AR grade
K_2CO_3	K_2O	10	99.9% pure, AR grade4
Boric Acid (H_3BO_3)	B_2O_3	7	99.5% pure, AR grade
NH_4F	F^-	4	95% pure, AR grade

FIGURES

Fig. 1: Components made of Machinable glass ceramics (www.precisionceramics.co.uk)

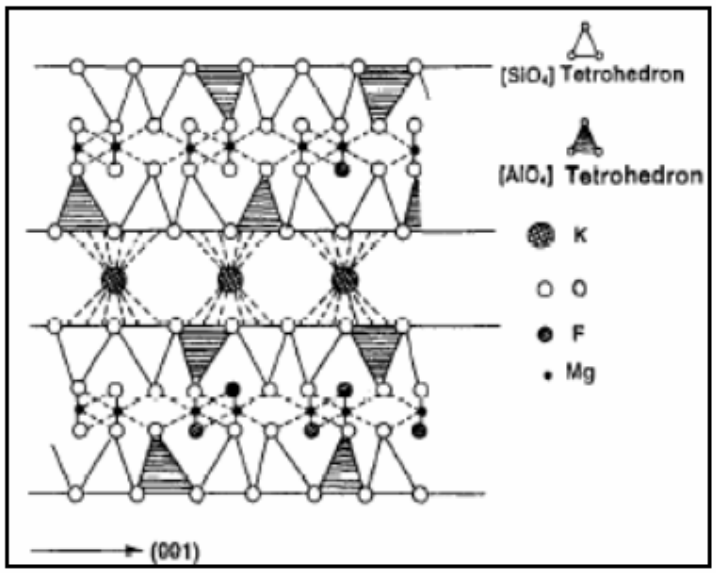

Fig.2: Schematic diagram showing the microstructure of fluorophlogopite (Chen et al [10])

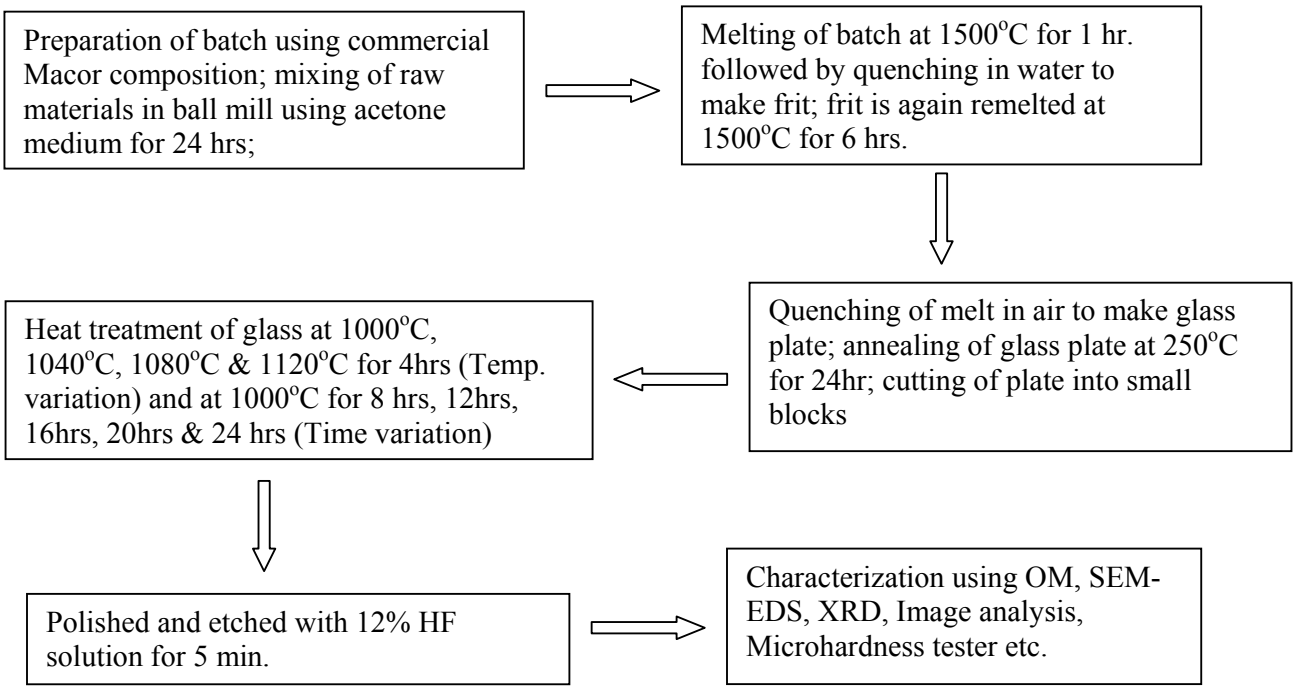

Fig.3: Flow chart describing the experimental procedure

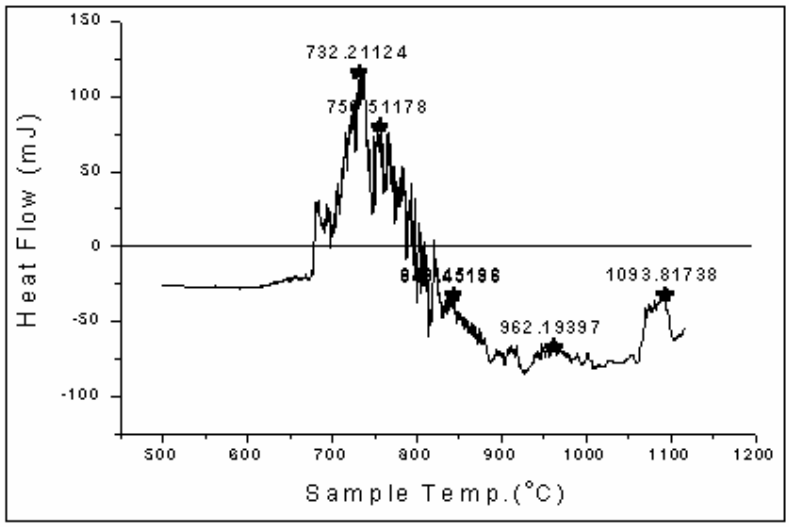

Fig.4: DTA diagram of the base glass

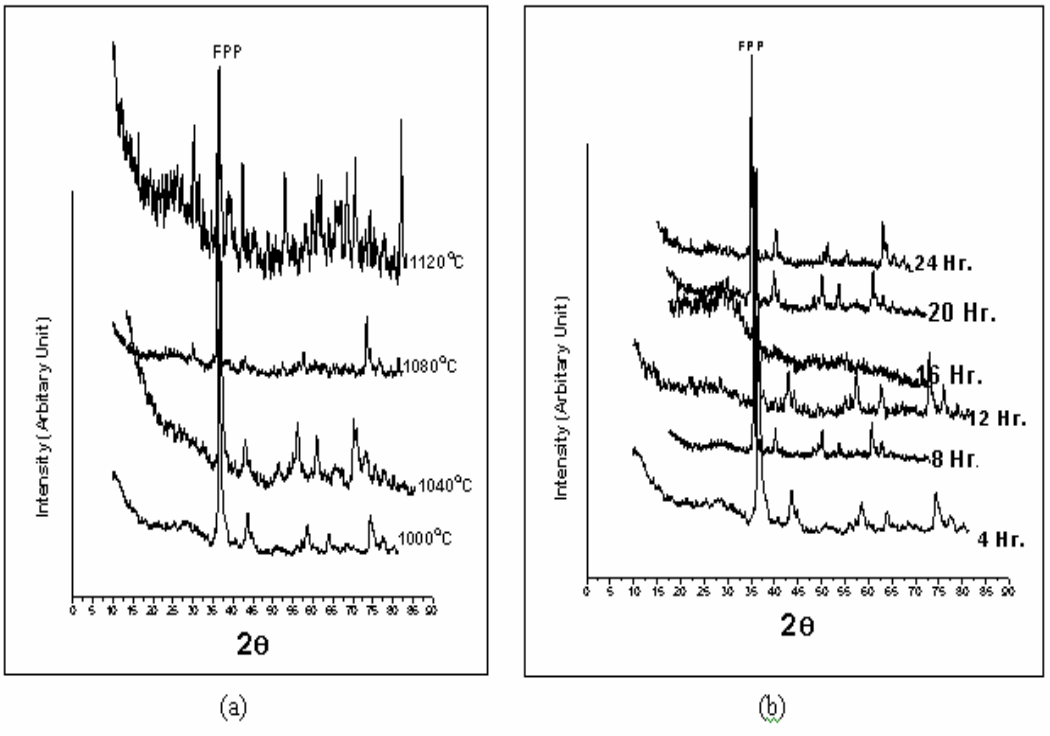

Fig 5: XRD spectra from (a) Temperature variation samples and (b) Time variation samples

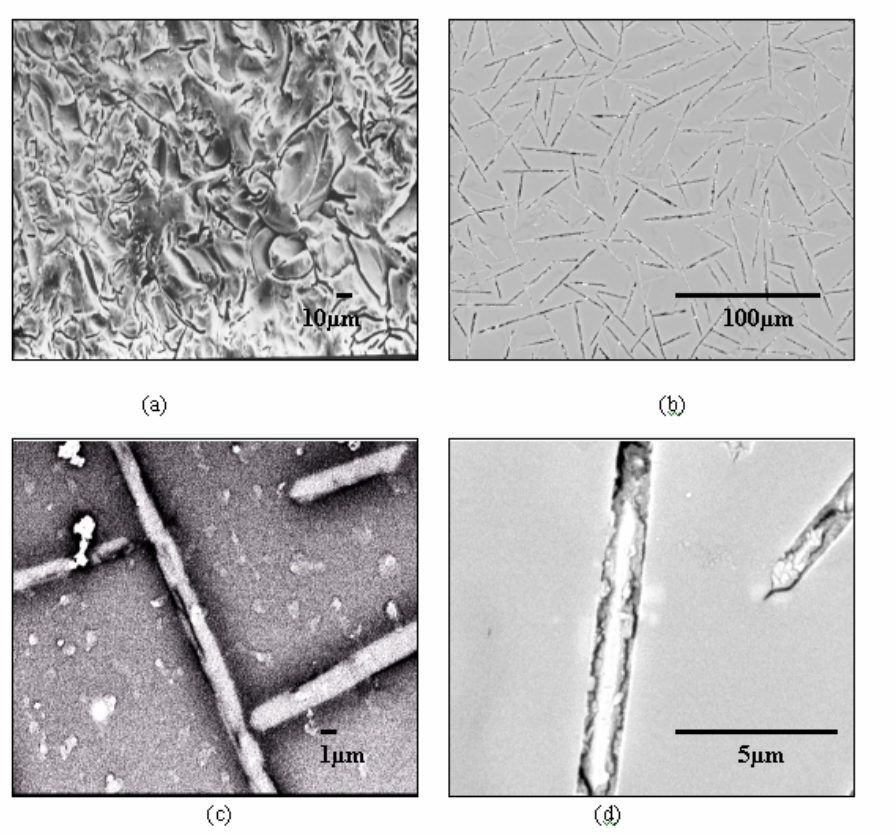

Fig.6: SEM micrograph of samples heat treated at (a) 1000^{o}C, 4 hrs, showing no sign of crystallinity, (b) 1120^{o}C, 4hrs showing usual randomly oriented interlocked mica flake, (c) 1120^{o}C, 4hr showing the interlocking between individual mica flakes and (d) 1120^{o}C, 4hr showing a single mica flake

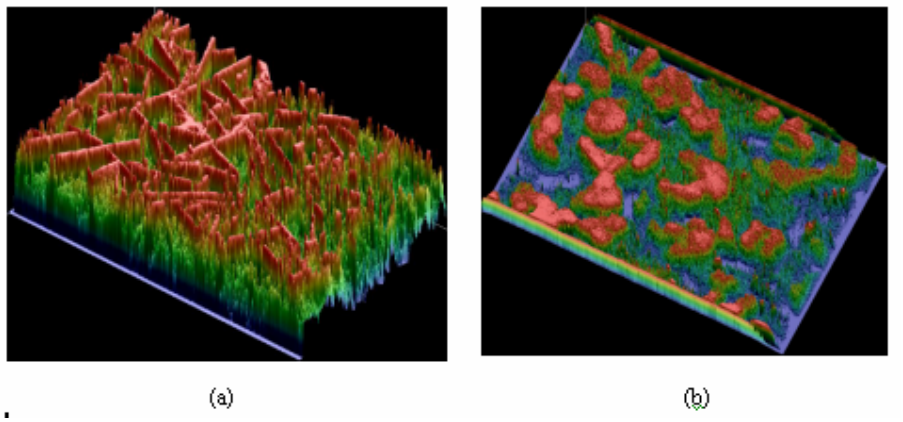

Fig.7: Surface plot of (a) temperature variation batches and (b) Time variation batches

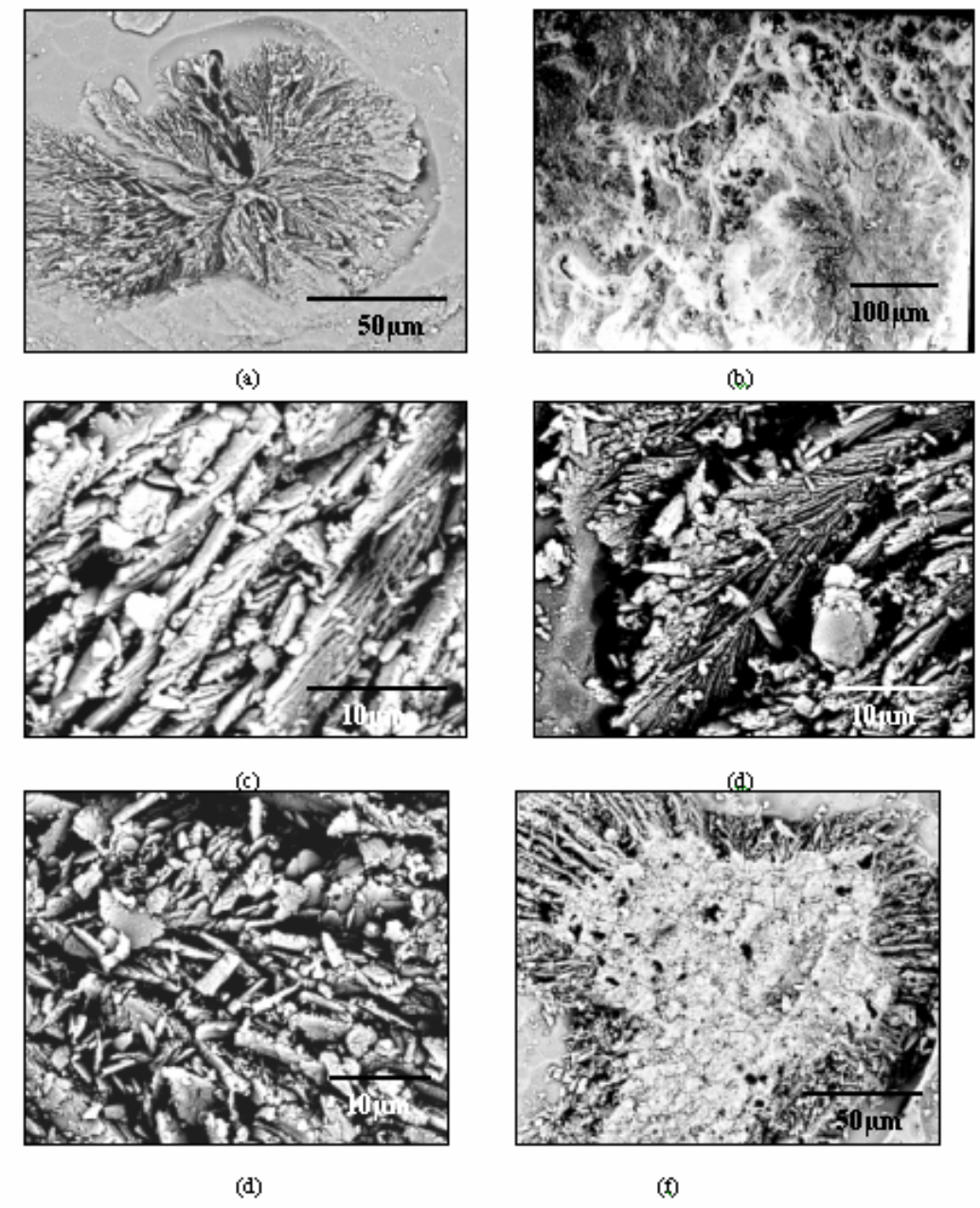

Fig.8: SEM micrographs of time variation samples showing (a) "Butterfly" shaped crystals, (b) Crystals are evolved from spherical droplets, (c) Stacking of mica plates forming mica rods, (d) "Tree leave" structure at the end of each mica rod, (e) Scattering of mica plates over the crystal phase, (f) Glassy patch over the crystal phase.

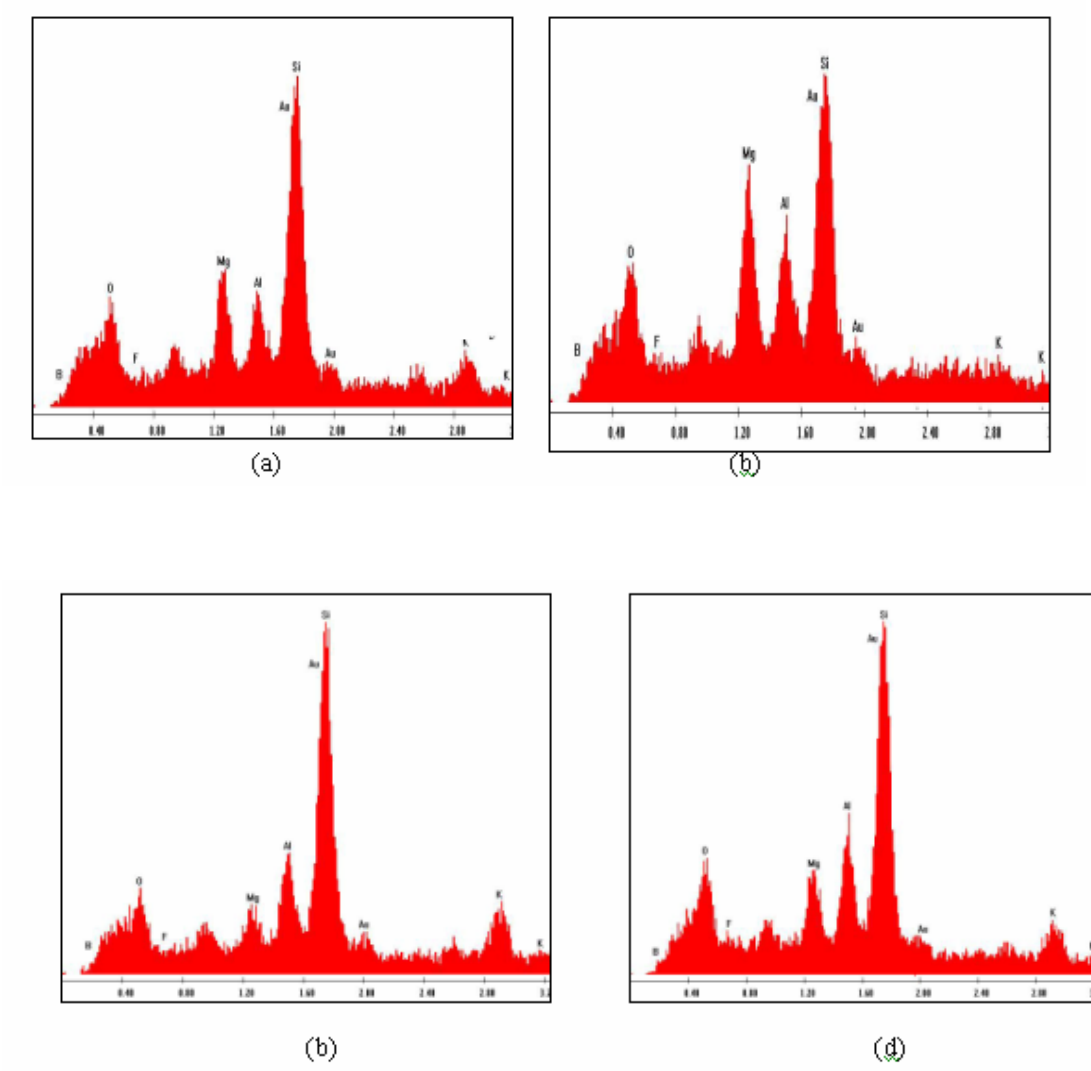

Fig.9: EDX diagrams of (a) & (b) crystals phases and (c) and (d) matrix phases of temperature and time variation samples respectively

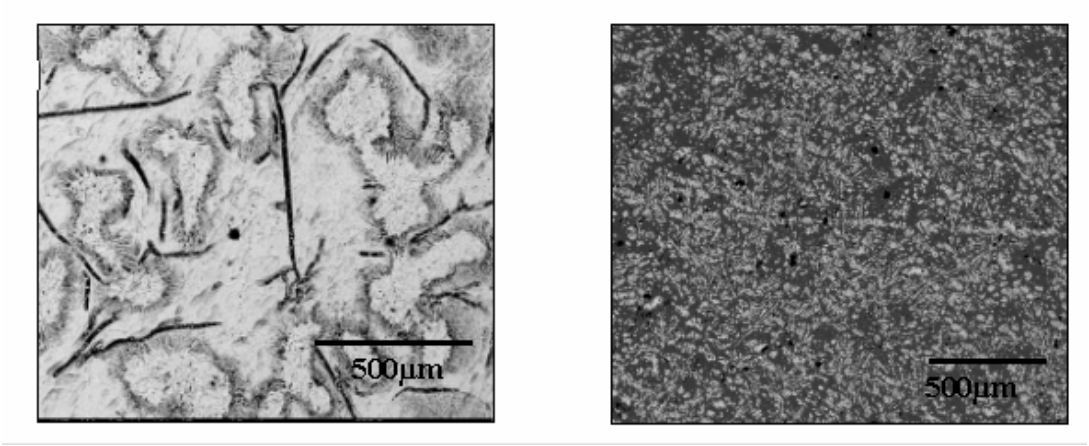

Fig.10: SEM micrographs of time variation samples showing (a) Overlapping of crystal phases for 20 hrs sample and (b) Confinement of glassy matrix within small isolated regions for 24 hrs sample

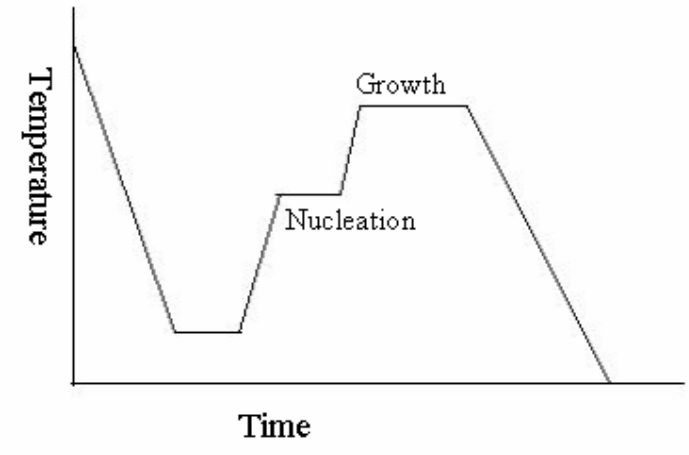

Fig.11: Heat treatment cycle showing time-temperature dependence in glass ceramic production

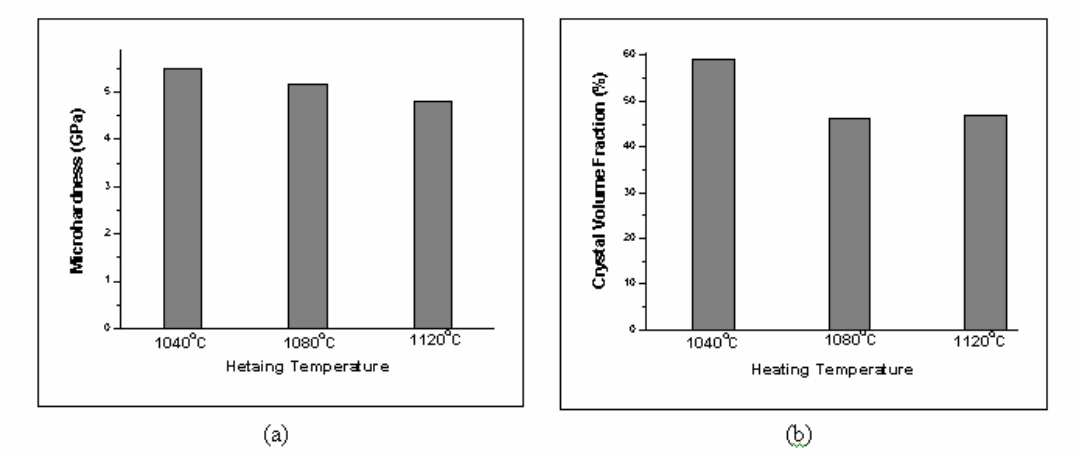

Fig.12: (a) Hardness and (b) Crystal volume fraction variation in temperature variation samples

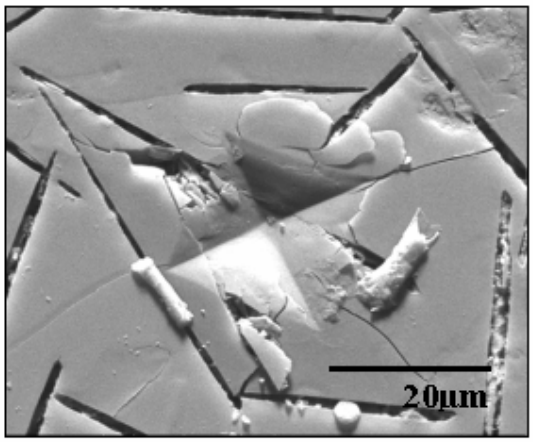

Fig.13: SEM micrograph of temperature variation samples showing indentation images without any deformation

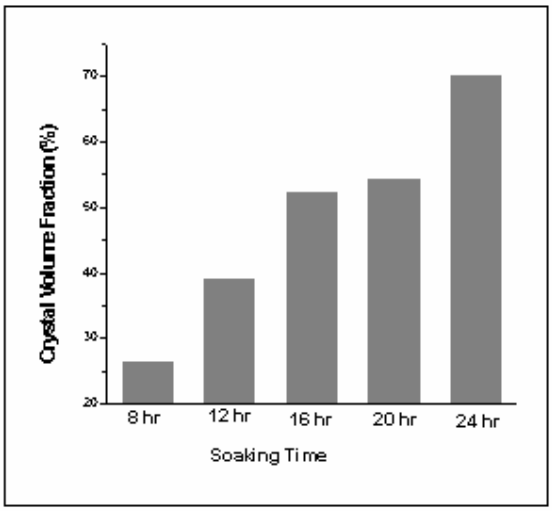

Fig.14: Crystal volume fraction in time variation samples

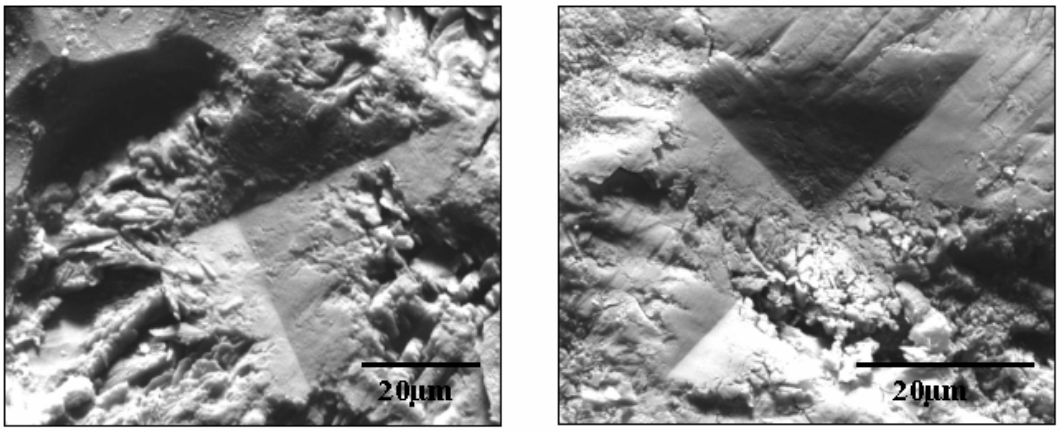

(a) (b)

Fig.15: SEM micrographs on time variation samples showing large deformation of the crystal pahse (a) 16hr samples, (b) 20hr samples